Adaptive Positioning Control for a LPMSM Drive Based on Adapted Inverse Model and Robust Disturbance Observer

Wei-Te Su and Chang-Ming Liaw, *Member, IEEE*

***Abstract*—The adaptive robust positioning control for a linear permanent magnet synchronous motor drive based on adapted inverse model and robust disturbance observer is studied in this paper. First, a model following two-degrees-of-freedom controller consisting of a command feedforward controller (FFC) and a feedback controller (FBC) is developed. According to the estimated motor drive dynamic model and the given position tracking response, the inner speed controller is first designed. Then, the transfer function of FFC is found based on the inverse model of inner speed closed-loop and the chosen reference model. The practically unrealizable problem possessed by traditional feedforward control is avoided by the proposed FFC. As to the FBC, it is quantitatively designed using reduced plant model to meet the specified load force regulation control specifications. In dealing with the robust control, a disturbance observer based robust control scheme and a parameter identifier are developed. The key parameters in the robust control scheme are designed considering the effect of system dead-time. The identification mechanism is devised to obtain the parameter uncertainties from the observed disturbance signal. Then by online adapting the parameters set in the FFC according to the identified parameters, the nonideal disturbance observer based robust control can be corrected to yield very close model following position tracking control. Meanwhile, the regulation control performance is also further improved by the robust control. In the proposed identification scheme, the effect of a nonideal differentiator in the accuracy of identification results is taken into account, and the compromise between performance, stability, and control effort limit is also considered in the whole proposed control scheme.**

***Index Terms*—Disturbance observer, feedforward controller (FFC), inverse model, linear permanent magnet synchronous motor (LPMSM), model reduction, parameter identification, position control, quantitative design, two-degrees-of-freedom controller (2DOFC).**

I. Introduction

THE high-precision and high-speed linear motor drives become increasingly important for manufacturing industries. As far as the direct linear motion driving is concerned, the positioning stages established using linear motors possess superior driving performance to those using rotary ones [1], [2]. Among the existing linear motors, the linear permanent magnet synchronous motor (LPMSM) is perhaps the most commonly employed one owing to its merits in high acceleration capability and high power density [1], [2]. As generally recognized, a motor driven positioning stage is an interdisciplinary system. To obtain satisfactory performance, it should have proper match between constituted components including motor, inverter, mechanical load, and control scheme. As far as the control issue is concerned, properly designed multiloop configured system consisting of current-controlled pulse-width modulation (PWM) scheme, velocity, and position loops is indispensable. Until now, many motion control methods have been developed for yielding better performance. The comparison and survey studies for some typical control methods can be found in [3]–[5].

From the survey for the existing researches [3]–[14], one can be aware that for achieving satisfactory motion control performance, the control scheme should consist of three components, namely feedback (FBC), feedforward (FFC), and disturbance cancellation controllers. Moreover, the tuning of controllers should also be considered. In [6], a one-degree-of-freedom acceleration tracking control scheme is augmented with an observer-based disturbance compensation controller. In [7], a two-degrees-of-freedom controller (2DOFC) is proposed, which consists of a proportional-plus-derivative (PD) FBC, a command FFC, a friction compensation FFC and a disturbance observer. As to the 2DOFC presented in [8], the states and disturbance are obtained from observer, and the FBC is designed employing optimal control approach. The stability preservation is handled by the FBC, and the steady-state error due to disturbance and uncertain modeling can be eliminated by the integral feedback control. However, this will introduce phase lag in servo tracking control and reduce the closed-loop phase margin. The application of observed disturbance cancellation control can reduce the feedback control demand and thus enhance the whole tracking control performance.

It is known that for achieving more robust control, the command feedforward control scheme should be adapted according to the varying plant behavior. An optimal hybrid FFC [9] and a learning FFC [10] have been developed to achieve this goal. In addition, there are still some existing control methods concerning the improvements of motion control, some of the typical ones can be referred to [11]–[21]. In [11], a multirate digital 2DOFC for hard disk driving control was proposed to yield specified tracking and disturbance rejection control requirements. These two tasks are specifically handled by the command feedforward and the FBCs. However, no robust control ability is found. In the 2DOFC presented in [12], it consists

Manuscript received August 25, 2004; revised May 31, 2005. Recommended by Associate Editor A. Emadi.

The authors are with the Department of Electrical Engineering, National Tsing Hua University, Hsinchu 300, Taiwan, R.O.C. (e-mail: cmliaw@ee.nthu.edu.tw)

Digital Object Identifier 10.1109/TPEL.2005.869729

of a feedforward compensator, a full-state FBC, and a radial basis function (RBF) self-tuning adaptive compensator. The FBC is designed using a linear quadratic regulator technique to preserve optimal and robust performance. The robust and quantitative positioning control for a linear brushless dc motor drive using a cascade 2DOFC and a disturbance robust control scheme was presented in [13]. Wherein the tuning of FFC is not performed. In [14], the authors performed the precision motion control for a PWM driven linear motor. In which, a third or higher-order low-pass filter is employed to generate the compensation control signal from the observed disturbance. However, the quantitative and robust control issues are not treated. In [15], the robust position control of manipulators in task space based on disturbance observer and inertia identifier was made. In its disturbance observer, the different compensation control generating functions are proposed to handle different types of disturbances. In the adaptive robust force control for linear synchronous motor made in [16], the environment stiffness is identified and used to adjust the parameters in the force FBC and the disturbance observer. However, the quantitative 2DOF control is not treated.

To improve the control performance of a disturbance observer (DOB) based positioning control scheme, an improved DOB, which is named as adaptive robust controller (ARC), is applied for machine tools [17]. The better tracking performance in the presence of discontinuous disturbances is achieved. The research made in [18] performed the nonlinear speed control for a permanent-magnet synchronous motor using improved disturbance estimation approach. The disturbance torque and flux linkage are simultaneously estimated, and then the motor control input voltages are computed accordingly to compensate the effects of nonlinear disturbances. However, this research treats only the speed control, and the positioning control is to be extended. Recently, in the motion control scheme proposed for direct-driven robot [19], an adaptive fuzzy disturbance estimator is designed to yield precise tracking control under unknown varying payload. In [20], a new robust tracking control scheme is developed. In order to suppress the sudden disturbance effect, a sudden disturbance observer is proposed. Finally, in [21], the basic feedback-feedforward 2DOFC is improved by adding a reference adjustment mechanism, which is used to learn and model the remnant tracking error and then modify the reference signal to yield improved tracking performance.

Generally speaking, there exist some key issues which are not yet totally solved by the existing methods in handling the motion control: i) the quantitative design approach to find the parameters of 2DOFC according to the given tracking and regulation control specifications; ii) the tuning control to let the control performance be insensitive to system parameter changes and disturbances; and iii) the design of FFC taking into account the realization feasibility and control demand. It is known that the disturbance observer based robust control schemes [6]–[8], [13]–[20] are very simple and effective in handling the compensation control against parameter variations and disturbances. However, the nonideal compensation caused by control effort limitation and system nonlinearities still can not be considered perfect.

This paper is mainly concerned with the adaptive robust positioning control for a LPMSM drive, considering the problems mentioned above. A DSP-based LPMSM drive is first established with its nominal dynamic model being estimated. Then, the robust and quantitative 2DOF motion control is performed. A reference model and an FFC based on adapted inverse model are employed to handle the tracking control problem. The inverse model used in the FFC is set considering the ease of realization, the resulting control effort and its parameters are updated online according to the estimated values. As to the regulation control, the FBC is designed according to the reduced-order plant model and the specified response. The effects of motor parameter variations, model reduction, and disturbances are reduced by the developed disturbance observer based robust control scheme and parameter identifier. The design of robust control scheme considering the effect of system dead-time is first made. Then, the nonideal robust disturbance cancellation control is corrected by the proposed self-tuning adaptive control approach. In the proposed identification scheme, the effects of system dead-time and nonideal differentiator are considered. In addition to the compensation control, the changes of motor drive parameters are identified from the observed disturbance, and they are used for tuning the parameters set in the FFC. Compromise between robust control performance, stability, and control effort is considered in the design stage of the proposed control scheme. Validity of the proposed control scheme is confirmed by simulated and experimental results.

II. DSP-Based LPMSM Drive

A. System Configuration

System configuration of the established DSP-based LPMSM driven stage is shown in Fig. 1. The LPMSM (manufactured by Normag Company, USA) is short-primary type. The ratings and system parameters of the LPMSM and inverter are listed in the Appendix . The ramp-comparison current-controlled PWM (CCPWM) scheme with switching frequency $f_s = 15$ kHz is designed to yield good current switching control performance. The current FBC of each phase winding is chosen to be PI type with its parameters being listed in the Appendix .

Normally, two sensors can only be employed for the motors with reasonably balanced three-phase currents. In this paper, three sensors are used for obtaining more accurate current sensing. In the situation of using two current sensors, many origins of error may exist in the synthesized current. Some key error origins include [22] the following. i) Nonsimultaneous measurements of two phase currents: for a three-phase ac motor, it is required to measure the currents in three motor windings at the same time exactly in order to get an instantaneous torque or force in the machine. Any time delay between the two measured currents will result in the error in the third synthesized current, and thus the whole motor driving control performance will be degraded accordingly. ii) dc offsets of current sensors: this may be due to the unbalanced voltage supplies for the sensing signal conditioners. iii) High-frequency leakage current in a PWM inverter-fed ac motor: the leakage current may flow through stray capacitance among stator windings and iron core of frame

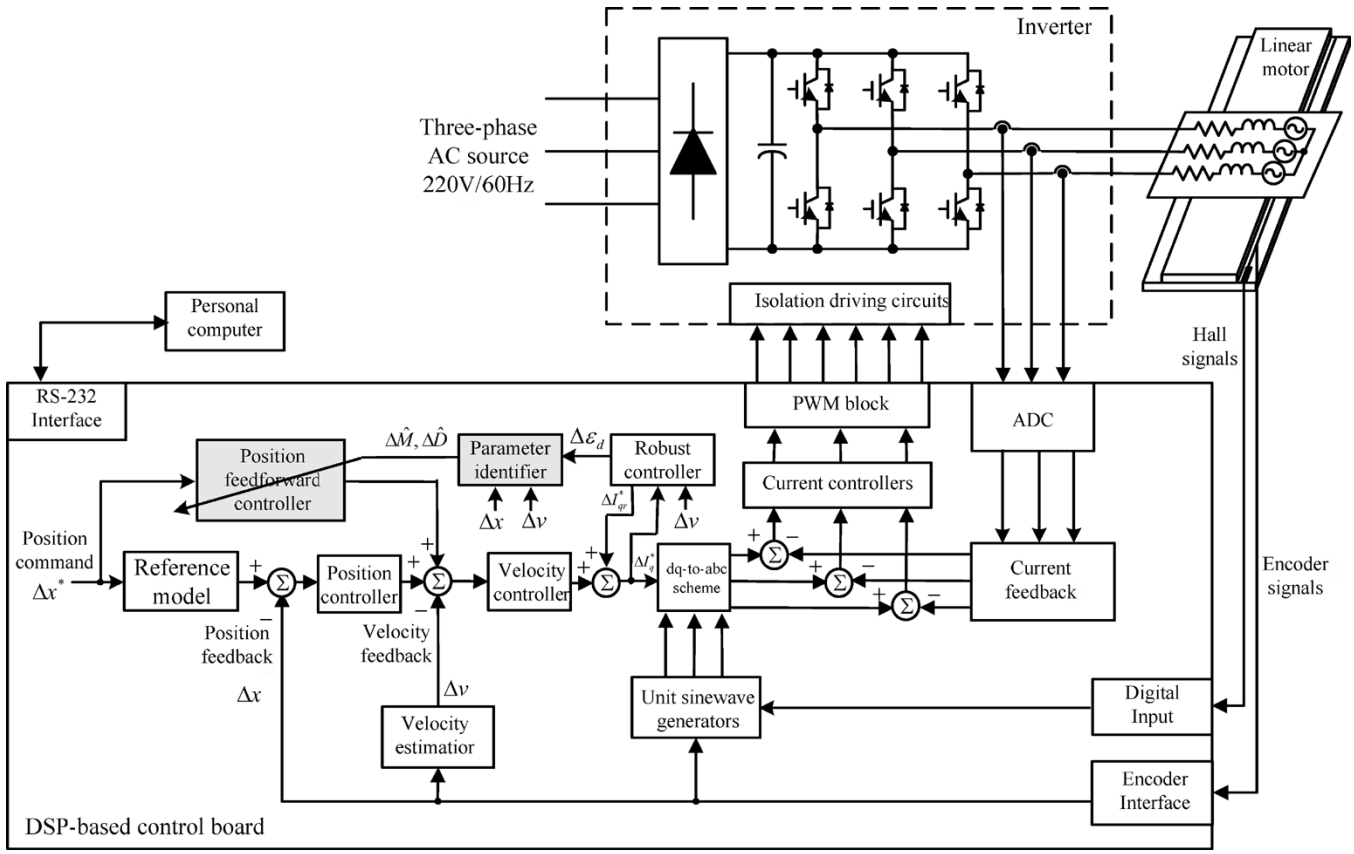

Fig. 1. System configuration of the established DSP-based LPMSM drive.

at the switching instants of inverter transistors. This will lead to the additional unbalance between three winding currents.

The DSP ADMC401 manufactured by Analog Devices Company is employed to establish the digital control environment. ADMC401 integrates a digital signal processor with a powerful array of memory-mapped motor control peripherals, including a 12-b simultaneous sampling ADC which provides eight analog inputs, a 16-b of six channels high resolution PWM scheme and two channels 8-b auxiliary PWM outputs, an incremental encoder interface, and event capture channels. The DSP provides a combination of efficient processing units such as a hardware MAC, an ALU, and shifter. Each instruction executes in a DSP cycle corresponding to 38.5 ns (i.e., 26 MIPs).

As generally recognized, adequate sampling rate selection significantly affects the digital control performance. The considerations include the tracking response smoothness, the disturbance rejection response, the stability, the effects of contaminated noises, the limit of word length representing the feedback variable, etc. The position, velocity, and current control loops of the established LPMSM drive shown in Fig. 1 are all fully realized digitally with the sampling rates of 1 kHz, 1 kHz and 30 kHz being properly chosen according to the given positioning control specifications, which will be described later in Section III. In addition, for the ac motor drive equipped with encoder speed sensor, the sampling rate of velocity loop should be chosen considering the resolution of the employed encoder. In the established motor drive, the resolution of encoder is 1 cm/10 000 counts. Careful derivation finds that the missing of one encoder count will lead to the velocity sensed errors of 0.1 cm/s and 1 cm/s for the sampling rates of 1 and 10 kHz, respectively. The adequacy of the 1-kHz sampling rate of speed loop for the adopted encoder is further verified.

The redesign approach is employed to find all digital control algorithms, and the bilinear method is used in making continuous- to discrete-time model transformation.

B. Dynamic Modeling of Position Loop

The electromagnetic developed force of a LPMSM drive and its mechanical equation can be written as [1], [13]

$$F_e = \frac{3}{2}\frac{P}{2}\frac{\pi}{\tau_p}\lambda_{\max} I_q \triangleq K_t I_q \approx K_t I_q^* = F_{Ld} + M\frac{dv}{dt} + Dv, v = \frac{dx}{dt} \tag{1}$$

where P is the pole number and τ_p the pole pitch, $\lambda_{\max}$ is the amplitude of the sinusoidal primary phase winding flux linkages caused by the permanent magnet in stationary secondary, K_t is the force generating constant, I_q is the q-axis current, I_q is the q-axis current command, $F_{Ld} \triangleq F_L + F_d$ is the composite force disturbances, F_L is the load force, F_d is the disturbance including cogging and reluctance forces, M is the mass of moving part, and D is the damping coefficient. In handling the motion control, it is assumed that d-axis current command $I_d^* = 0$ is set and $I_q \approx I_q^*$ for the close current tracking characteristics. According to (1), the control system block diagram is drawn in

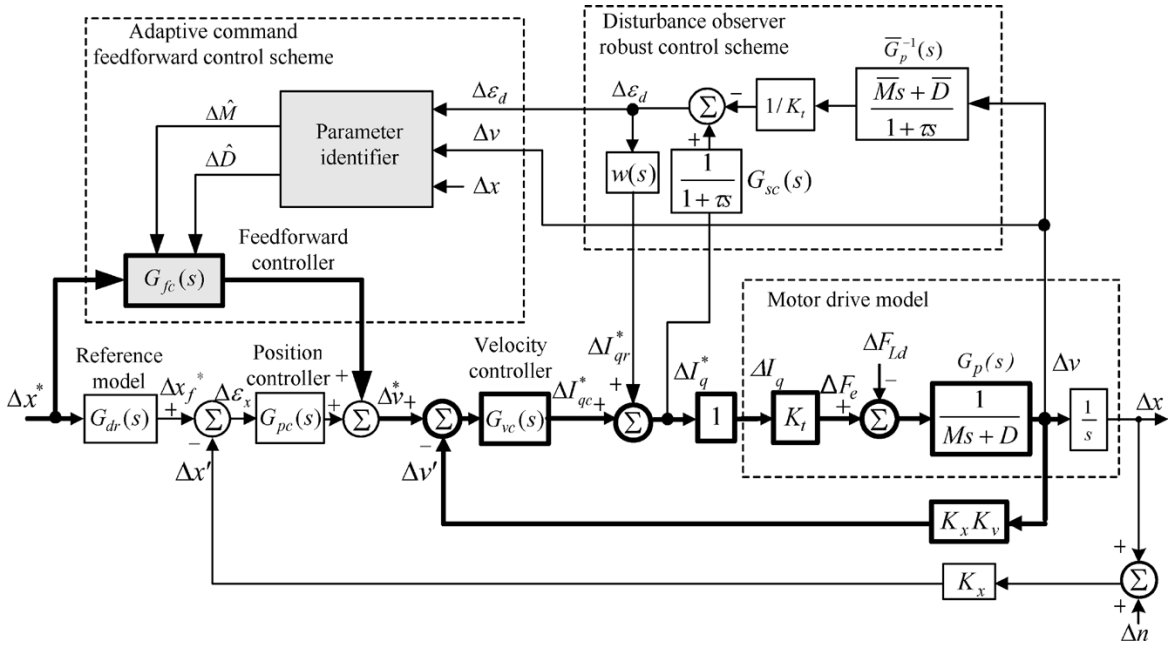

Fig. 2. Proposed control scheme.

Fig. 2. For the convenience of derivation, the parameters of the plant model $G_p(s)$ are defined as

$$G_p(s) = \frac{\Delta v}{\Delta F_e} = \frac{1}{Ms + D} \triangleq \frac{b}{s + a},\ a = \frac{D}{M},\ b = \frac{1}{M}. \tag{2}$$

The sensing factors K_x =100 and $K_v = 0.1$ are set to let the scaling of position Δx be 1 cm to 1 V and the scaling of velocity Δv be 10 cm/s to 1 V, respectively.

Since the accurate dynamic model is not easy to obtain via physical derivation, the step-response estimation approach [13], [23] is employed to find the estimates of dynamic model parameters. Detailed estimation procedure can be referred to [13], [23]. The estimated parameters are

$$D = 56.875\ \frac{\text{kg}}{\text{s}},\ \ M = 4.55\ \text{kg},\ \ K_t = 35.44\ \frac{\text{Nt}}{\text{A}}. \tag{3}$$

III. Proposed Control Scheme

The proposed control scheme shown in Fig. 2 consists of a P-type velocity controller $G_{vc}(s)$, a position 2DOFC, a disturbance observer robust control scheme, a signal conditioning compensator $G_{sc}(s)$ and a parameter identifier. The 2DOFC further consists of a FBC $G_{pc}(s)$, an adaptive command FFC $G_{fc}(s)$, and a reference model $G_{dr}(s)$. Due to the close current tracking control being achieved, $\Delta I_q \approx \Delta I_q^*$ is assumed in handling the positioning control. The design methodology of the proposed 2DOFC is that $G_{vc}(s)$ and $G_{pc}(s)$ are emphasized on handling the quantitative load regulation control, and $G_{fc}(s)$ and $G_{dr}(s)$ are employed to obtain the desired command tracking response. It is well known that the tracking control can be much improved via applying command FFC. However, the FFC in most existing control schemes [3]–[8], [11]–[17] possesses the practical realization problem owing to the need of differentiation. In the proposed FFC, its transfer function is formed from the inverse model of inner speed closed-loop and the chosen reference model. The later derivation will find that the differentiation can be avoided in the designed FFC. Furthermore, in addition to the stability preservation, the FBC is quantitatively designed according to the plant model and the given regulation control requirements. Although the disturbance observer based robust control approaches [6]–[8], [13]–[20] are effective in the rejection control for the disturbance and parameter changes, the ideal cancellation control is generally impossible to achieve. The difficulties lie in the existence of control effort limitation, the parameter variations, the nonideal differentiator being employed, the effect of system dead-time, etc. It has also been found that the control performance can be much improved, if the constituted controllers can be online adapted their parameters. In some existing research, the tuning of FFCs [9], [10], [15] and FBC [16] based on the identified plant key parameters and variables have been made.

In this paper, the disturbance observer based robust control scheme is employed to reduce the effects of system parameter variations and disturbances. The robust control performance is determined by choosing a suited weighting function $w(s)$ considering the effects of system dead-time. Then, the nonideal robust cancellation control is improved by the developed self-tuning adaptive control scheme. In which, an identifier is employed to yield the estimates of mechanical parameter changes from the observed disturbance, and they are then used to update the ones being set in $G_{fc}(s)$, such that excellent tracking performance under varying plant can be obtained.

The roles of the constituted components in the proposed control scheme can be comprehended from the design procedures introduced as follows. While the design at nominal case is first described here, the robust control against the system parameter variations will be presented in the next section. As generally recognized, the low-pass filter approach is employed to realize the differentiator in the inverse plant model $\overline{G}_p^{-1}(s)$ used in the

disturbance observer [6]–[8], [13]–[20]. To avoid the error in the estimated disturbance $\Delta\varepsilon_d$, the signal conditioning compensator $G_{sc}(s) = 1/(1+\tau s)$ shown in Fig. 2 is added in the disturbance observer. It should be noted that if there exist system nonlinearities, such as dead-time element, limiter, etc., their transfer functions should also be added in $G_{sc}(s)$.

A. Summary

In short, compared with the existing 2DOFC and disturbance observer based robust control schemes [3]–[21], the main features of the proposed control schemes can be summarized as: i) without using the differentiator in the developed command FFC, ii) having quantitative and robust control performances in the designed 2DOFC, iii) the command FFC is online adjusted its parameters according to the identified system parameters, iv) a parameter identifier using estimated disturbance signal is developed, v) the effect of nonideal differentiator used in the disturbance observer based robust control scheme is compensated, and vi) the dead-time effect is considered in the key parameters determination of the robust controller. The last four features will be comprehended in the next section.

B. Tracking Control

The step-response specifications are given as: i) no over-shoot, ii) no steady-state error, and iii) response time $t_{rc} = 0.05$ s, which is defined as the response at which it is equal to 90% of its steady-state value.

1) Speed Controller: The P-type velocity FBC is chosen

$$G_{vc}(s) = K_{vp}. \tag{4}$$

By neglecting the robust control scheme and employing the nominal system parameters, the velocity closed-loop transfer function can be derived from Fig. 2 to be

$$\begin{aligned} G_{vr}(s) &\triangleq \left.\frac{\Delta v'}{\Delta v^*}\right|_{\Delta F_{Ld}(s)=0} = \frac{K_x K_v K_t \overline{b} K_{vp}}{s + (\overline{a} + K_t \overline{b} K_{vp} K_x K_v)} \\ &\triangleq \frac{K_x K_v K_t \overline{b} K_{vp}}{s + \mu_v} \end{aligned} \tag{5}$$

where $\overline{a} \triangleq \overline{D}/\overline{M}$ and $\overline{b} \triangleq 1/\overline{M}$. Generally, the pole μ_v can be set to let the response speed of velocity-loop is about ten-times of position-loop. By letting $\mu_v = 10/t_{rc} = 200$ and using the parameters given previously, one can find $K_{vp} = 2.407$ from (5).

2) Command FFC: The desired tracking response is defined by the reference model $G_{dr}(s)$. It follows from Fig. 2 that the command FFC is naturally set as

$$G_{fc}(s) = G_{dr}(s) G_{vr}^{-1}(s) \frac{s}{K_x}. \tag{6}$$

Obviously, many types of transfer functions for $G_{dr}(s)$ can satisfy the desired response. To facilitate the realization of $G_{fc}(s)$, the reference model $G_{dr}(s)$ is chosen as a second-order critically-damped system

$$G_{dr}(s) = \left(\frac{\mu_{dr}}{s + \mu_{dr}}\right)^2. \tag{7}$$

The unit-step time response of (7) and its derivative are

$$y(t) = 1 - (1 + \mu_{dr} t) e^{-\mu_{dr} t} \tag{8}$$

$$\frac{dy(t)}{dt} = \mu_{dr}^2 t e^{-\mu_{dr} t}. \tag{9}$$

From (8) and (9), one can find that the time response has no over-shoot and steady-state error. For the given tracking specifications, one can find that the repeated pole of $G_{dr}(s)$ can be solved from the following equation:

$$0.9 = 1 - (1 + \mu_{dr} t_{rc}) e^{-\mu_{dr} t_{rc}} \tag{10}$$

to be $\mu_{dr} = 77.7944$.

Realization Issue

The transfer function $G_{fc}(s)$ can be found from (5)–(7) to be

$$\begin{aligned} G_{fc}(s) &= \frac{\mu_{dr}^2 \left[s^2 + (a + K_{vp} K_t b K_x K_v) s\right]}{K_{vp} K_t b K_x (s + \mu_{dr})^2} \\ &= \frac{\mu_{dr}^2 \overline{M} s^2 + \mu_{dr}^2 (\overline{D} + K_{vp} K_t K_x K_v) s}{K_{vp} K_t K_x (s + \mu_{dr})^2}. \end{aligned} \tag{11}$$

One can be aware from (11) that the command FFC $G_{fc}(s)$ developed here does not contain a pure derivative. This is a common problem in realization for most of the existing conventional command FFCs [3]–[8], [11]–[17].

Parameter Adaptation

Under varying operating conditions, the parameters $\overline{M}$ and $\overline{D}$ being set in (11) will not again lead to the satisfactory command feedforward control. Thus, the parameter adaptation is necessary to yield excellent model following tracking response. In this paper, the disturbance observer robust control is applied to reduce the parameter changes. These parameter changes are simultaneously identified by the proposed identification scheme and used to update the parameters set in the $G_{fc}(s)$. The nonideal disturbance observer robust cancellation control can be corrected automatically. Detailed derivations of the proposed robust control and self-tuning adaptive control approaches will be presented in the next section.

Control Effort

The closed-loop transfer function from control force to command can be derived from Fig. 2 as (12), shown at the bottom of the next page. The maximum control force for unit-step command change (1 cm), which occurs at $t = 0$, can be found from (12) and (7) as

$$I_{q,\max} = \frac{\mu_{dr}^2}{K_t b K_x} = \frac{\overline{M} \mu_{dr}^2}{K_t K_x}. \tag{13}$$

Thus, obviously, the maximum current is proportional to μ_{dr}^2. According to the reference-frame theory, one can find that $I_{q,\max}$ is equal to the maximum phase winding current at initial transient. However, the duration of this current is very short. Applying the known system parameters, $I_{q,\max} = 7.77$ A is found for a step command change of 1 cm.

Natural Frequency

From (7) one can find another expression of the desired closed-loop tracking transfer function

$$H_{dr}(s) \triangleq \left.\frac{\Delta x'(s)}{\Delta x^*(s)}\right|_{\Delta F_{Ld}(s)=0} = G_{dr}(s) = \frac{\mu_{dr}^2}{s^2+2\mu_{dr}s+\mu_{dr}^2} \triangleq \frac{\omega_n^2}{s^2+2\xi\omega_n s+\omega_n^2} \quad (14)$$

which is a second-order system with unity damping ratio and natural frequency $\omega_n = \mu_{dr} = 77.7944$ rad/s.

C. Regulation Control

The position FBC $G_{pc}(s)$ is in charge of handling quantitative load regulation control and meanwhile the tracking error regulation. The position response characteristics for unit-step load force change ($1N - m \Rightarrow 1N$) are specified as: i) zero steady-state error and over-shoot, ii) maximum dip $\Delta x_m = 10\ \mu$m, and iii) restore time $t_{rd} = 0.1$ s, which is defined as the position response at which it is equal to $0.1\Delta x_m$ (i.e., $\Delta x(t = t_{rd}) = 0.1\Delta x_m$). $G_{pc}(s)$ is chosen as

$$G_{pc}(s) = K_{pp} + \frac{K_{pi}}{s}. \quad (15)$$

The closed-loop regulation transfer function can be derived from Fig. 2 as (16), shown at the bottom of the page, where

$$c_1 \triangleq bK_x = 21.98 \quad (17)$$

$$d_2 \triangleq a + K_{vp}K_t bK_x K_v = 171.4647 \quad (18)$$

$$d_1 \triangleq K_{pp}K_{vp}K_t bK_x = 1589.6465K_{pp} \quad (19)$$

$$d_0 \triangleq K_{pi}K_{vp}K_t bK_x = 1589.6465K_{pi}. \quad (20)$$

Basically, there are two approaches to handle the regulation control quantitatively: i) the governing equations relating response characteristics, the parameters of position PI FBC and speed P FBC are derived from (16), and three parameters of these two controllers are solved. Then the transfer function of FFC is found following the procedure presented above, and ii) the proportional gain of speed FBC is first designed as above. And then in the design of $G_{pc}(s)$, a second-order reduced model of $H_{dd}(s)$ is found and the quantitative design of the PI-type position FBC is made accordingly. The latter approach is adopted here.

Suppose that the transfer function of $H_{dd}(s)$ is approximated by

$$H_{dd}(s) \approx H'_{dd}(s) = \frac{-c'_1 s}{d'_2 s^2 + d'_1 s + d'_0} \triangleq \frac{-b_1 s}{(s+a_1)(s+a_2)} \quad (21)$$

where $-b_1 s/[(s+a_1)(s+a_2)]$ denotes the desired regulation response transfer function. The model reduction affair is first treated. As generally recognized, there have been many existing model reduction methods [24]. Among these, the time-moment and/or Markov parameter matching approaches are the most intuitive and easiest ones. While the first approach is emphasized on the low-frequency response matching, the latter one can lead to closer response matching in the high-frequency range.

By applying time-moment matching to (21), one naturally can find that $c'_1 = c_1$, $d'_2 = d_2$, $d'_1 = d_1$ and $d'_0 = d_0$, respectively. However, the initial transient response of the reduced-order model will be deviated from the original one significantly. To improve this, it is suggested to let c'_1 and d'_2 of $H'_{dd}(s)$ be found by matching the frequency response of $H'_{dd}(s)$ to those of $H_{dd}(s)$ at a high frequency, which is chosen at $\omega = \omega_n$, with ω_n being the natural frequency of the desired position tracking transfer function listed in (14). From (16) and (21) letting

$$H_{dd}(s = j\omega_n) = H'_{dd}(s = j\omega_n) \quad (22)$$

and through careful derivation one can find

$$c'_1 = \frac{c_1 d_1}{d_1 - \omega_n^2},\ d'_2 = \frac{d_0 - d_1 d_2}{\omega_n^2 - d_1},\ d'_1 = d_1,\ d'_0 = d_0 \quad (23)$$

$$a_1 + a_2 \triangleq \frac{d'_1}{d'_2},\ a_1 a_2 \triangleq \frac{d'_0}{d'_2},\ b_1 \triangleq \frac{c'_1}{d'_2}. \quad (24)$$

The position response due to the unit-step load force change can be found from (21) as

$$x_{dd}(t) = \frac{-b_1}{(a_1 - a_2)}\left(a_1 e^{-a_1 t} - a_2 e^{-a_2 t}\right). \quad (25)$$

$$H_{di}(s) \triangleq \left.\frac{\Delta I^*_{qc}(s)}{\Delta x^*(s)}\right|_{\Delta F_{Ld}(s)=0} = \frac{G_{dr}(s)}{K_t bK_x} \cdot \frac{s^5 + (K_{vp}K_t bK_x K_v + 2a)s^4 + (a^2 + K_{vp}K_t bK_x K_v a + K_{pp}K_{vp})s^3 + K_{vp}(K_{pi} + K_{pp}a)s^2 + K_{pi}K_{vp}as}{s^3 + (a + K_{vp}K_t bK_x K_v)s^2 + K_{pp}K_{vp}K_t bK_x s + K_{pi}K_{vp}K_t bK_x} \quad (12)$$

$$H_{dd}(s) \triangleq \left.\frac{\Delta x'(s)}{\Delta F_{Ld}(s)}\right|_{\Delta x^*(s)=0} = \frac{-bK_x s}{s^3 + (a + K_{vp}K_t bK_x K_v)s^2 + K_{pp}K_{vp}K_t bK_x s + K_{pi}K_{vp}K_t bK_x} \triangleq \frac{-c_1 s}{s^3 + d_2 s^2 + d_1 s + d_0} \quad (16)$$

The maximum position dip Δx_m and the time instant t_m when it occurs can be derived from the following two equations:

$$\Delta x_m = \frac{-b_1}{(a_1 - a_2)} \left(a_1 \left(\frac{a_1}{a_2} \right)^{-2a_1/(a_1 - a_2)} - a_2 \left(\frac{a_1}{a_2} \right)^{-2a_2/(a_1 - a_2)} \right) \tag{26}$$

$$t_m = \frac{2 \ln \left(\frac{a_1}{a_2} \right)}{a_1 - a_2} \tag{27}$$

and the restore time t_{rd} can be found from

$$x_{dd}(t_{rd}) = 0.9 \Delta x_m = \frac{-b_1}{(a_1 - a_2)} \left(a_1 e^{-a_1 t_{rd}} - a_2 e^{-a_2 t_{rd}} \right). \tag{28}$$

Based on (26)–(28), one can construct the following nonlinear equations:

$$f_1(a_1, a_2) = \Delta x_m - \frac{-b_1}{(a_1 - a_2)} \times \left(a_1 \left(\frac{a_1}{a_2} \right)^{-2a_1/(a_1 - a_2)} - a_2 \left(\frac{a_1}{a_2} \right)^{-2a_2/(a_1 - a_2)} \right) \tag{29}$$

$$f_2(a_1, a_2) = 0.9 \Delta x_m - \frac{-b_1}{(a_1 - a_2)} (a_1 e^{-a_1 t_{rd}} - a_2 e^{-a_2 t_{rd}}). \tag{30}$$

From (23), (24), and (17)–(20) one can find that f_1 and f_2 are nonlinear functions of two independent variables K_{pp} and K_{pi}. Thus, for the specified response parameters $\Delta x_m = 10\ \mu$m and $t_{rd} = 0.1$ s, K_{pp} and K_{pi} can be solved using the available Matlab software as

$$G_{pc}(s) = 11.7927 + \frac{300.7061}{s}. \tag{31}$$

D. Results

The simulated position, velocity and current responses due to a position step command change of 0.1 cm by the designed 2DOF controller at nominal case ($M = \overline{M}$) are shown in Fig. 3(a). The key parameters in these responses completely meet the specified ones. Fig. 3(b) shows the simulated responses due to a step load force change of 1 Nt, wherein the position trace denoted by "b" on the first plot of Fig. 3(b) represents the result yielded by reduced model, i.e., the specified response, and the trace "a" represents the actual position response. The results in Fig. 3(b) show that the actual position response is close to the specified one. The little difference caused by model reduction will be regarded as an unmodeled disturbance, and its effect will be reduced via robust control.

The measured tracking at the same conditions of Fig. 3(a) are plotted in Fig. 4(a). The results show that they are very close to the simulated ones. Fig. 4(b) plots the measured responses due to a step load force change of 5.316 Nt. The measured results are divided by a factor of 5.316 to yield the results due to unit-step

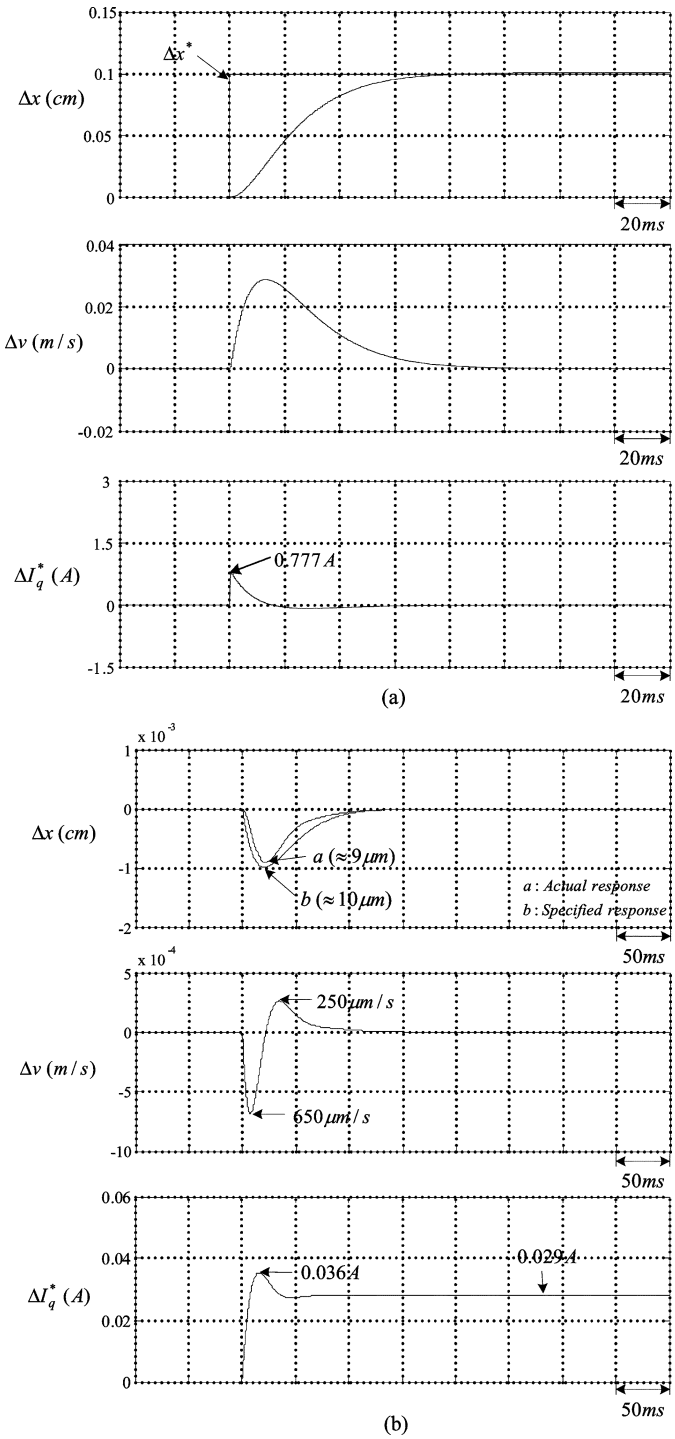

Fig. 3. Simulated results at nominal case ($M = \overline{M}$): (a) responses due to a step command change of 0.1 cm and (b) responses due to a step load change of 1 Nt.

load force change. The comparison between the converted measured and simulated unit-step load regulation responses find the following key parameters: i) maximum position dip: simulated $= 9\ \mu$m, measured $= 8.2\ \mu$m; ii) negative and positive values of Δv: simulated $= (-650\ \mu\text{m/s}, +250\ \mu\text{m/s})$, measured $= (-470\ \mu\text{m/s}, +470\ \mu\text{m/s})$; and iii) peak and steady-state values of ΔI_q^*: simulated $= (0.036$ A, 0.029 A), measured $= (0.049$ A, 0.028 A). One can find that these two types of results are rather similar in waveform shapes and possess some

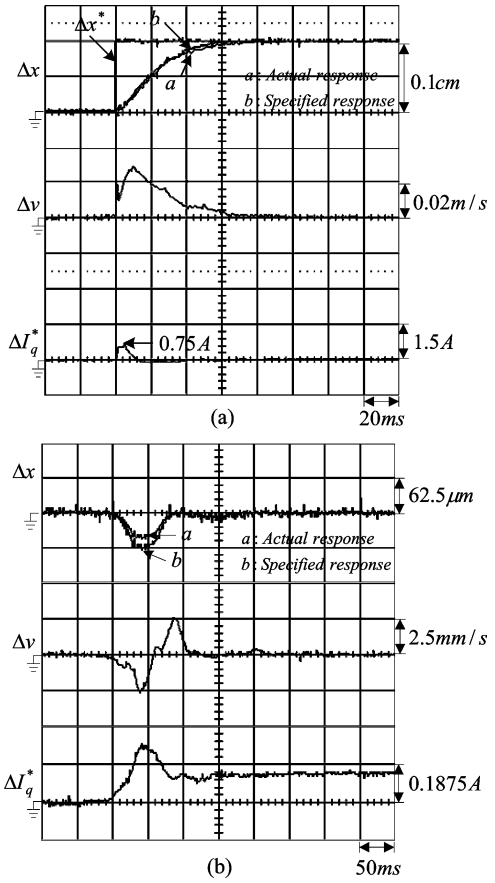

Fig. 4. Measured results at nominal case ($M = \overline{M}$): (a) responses due to a step command change of 0.1 cm and (b) responses due to a step load change of 5.316 Nt.

differences in the peak values of Δv and ΔI_q^*. The key reason lies in the fact that the applied load force change in measurement is not an ideal step function.

IV. Robust Disturbance Cancellation and Adaptive Feedforward Controls

Generally, a high performance positioning motor drive must have robust control performance. The 2DOF controllers developed above can match the desired specifications only at nominal case. As the changes of plant parameters and operating condition occur, the previously designed 2DOFC with fixed parameters can not further preserve the specified control requirements. Until now, although a lot of improved control techniques [3]–[21] have been developed, there still exist some key issues to be studied further. According to the survey for the existing control techniques, one can find that the observer based robust control scheme [6]–[8], [13]–[20] is perhaps the easiest one. However, the excellent compensation control for the uncertainties and disturbances is still difficult to obtain.

To let the proposed 2DOFC possess adaptability and robustness against parameter uncertainties and disturbance, a robust control parameter identifier is developed, and the adaptation of command FFC is performed according to the identified parameters. Configuration of the proposed control scheme is shown in Fig. 2, and the design of its constituted components is presented

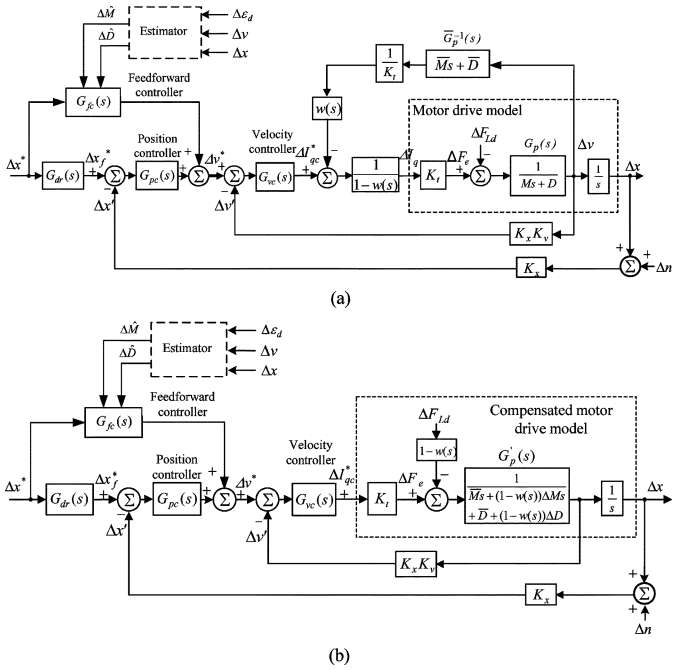

Fig. 5. (a) Alternative expression of Fig. 2 and (b) equivalent control system block diagram of (a) being viewed from the speed loop output.

as followed. Compared with the existing ones, the proposed control scheme possesses many salient features, which have been mentioned in the previous section.

A. Robust Control and Identification Schemes

In the disturbance robust control scheme shown in Fig. 2, an inverse nominal plant model $\overline{G}_p^{-1}(s)/K_t = (\overline{M}s+\overline{D})/K_t(1+\tau s)$ is utilized to extract the disturbance estimate $\Delta\varepsilon_d$, where the s is replaced by $s/(1+\tau s)$ to resolve its physical realization problem. And a simple compensator $G_{sc}(s) = 1/(1+\tau s)$ is added to yield accurate parameter estimates. A weighted compensation control signal $\Delta I_{qr}^* = w(s)\Delta\varepsilon_d$, $w(s) = w/(1+\tau s)$, $0 \le w \le 1$, is generated. Where the weighting factor w is chosen considering the compromise between the required control effort and the control performance, and the 1st-order low-pass filter set in $w(s)$ is employed to reduce the current command changing rate and the effect of high-frequency noise on the robust control operation. In this paper, according to the sampling rate of 1 kHz being chosen for the speed loop, $\tau =$ 1 ms is chosen. The effects of the nonideal differentiation on the parameter identification and the robust control performance are considered in the proposed control scheme. An alternative expression of Fig. 2 is drawn in Fig. 5(a). For ease of analysis, the ideal inverse plant model is considered. One can find from Fig. 5(a) that the existence of equivalent high gain $(1/(1-w(s))$ may significantly affect the stability and performance of the robust control system. A practical design to deal with these problems will be presented later in this paper.

Suppose that i) the mechanical mass and the damping ratio are subject to the variations of ΔM and ΔD (i.e., $M \triangleq \overline{M} + \Delta M$ and $D \triangleq \overline{D} + \Delta D$) and ii) the force generating constant $K_t \approx$ constant for the permanent magnet linear motor. Through careful derivation from Fig. 5(a) one can find that the

compensated motor drive model viewed from the speed loop output can be expressed as

$$K_t\Delta I_{qc}^* = [\overline{M}+(1-w(s))\Delta M]s\Delta v+[\overline{D}+(1-w(s))\Delta D]\Delta v +(1-w(s))\Delta F_{Ld}. \quad (32)$$

Accordingly, Fig. 5(a) can be reduced to those shown in Fig. 5(b). Equation (32) and Fig. 5(b) show that all the system disturbance and uncertainties have been reduced their effects by a frequency-dependent factor of $(1-w(s))$.

The control effort found from Fig. 5(a) is

$$\Delta I_q \approx \Delta I_q^* = \frac{1}{1-w(s)}\left(\Delta I_{qc}^* - \frac{w(s)}{K_t}(\overline{M}s+\overline{D})\Delta v\right). \quad (33)$$

If a scalar weighting factor, i.e., $w(s) = w$ is chosen, one can find that the maximum value of ΔI_q^*, which occurs at $t = 0$, will become larger for the value of w being closer to 1. And ΔI_q^* becomes impulse when $w = 1$ is set for achieving ideal robust cancellation control. If the frequency-dependent weighting function $w(s) = w/(1+\tau s)$ is chosen, the similar phenomena are also observed except that the peak value of ΔI_q^* will occur at the time instant $t > 0$. For the proposed control scheme, a reasonably large value of w (<1) is chosen to avoid the inherent problems possessed by the conventional robust disturbance cancellation control scheme, and the excellent tracking control is achieved via real-time tuning the command FFC. It follows that under the varied case ($M = \overline{M} + \Delta M$, $D = \overline{D} + \Delta D$) with perfect model following tracking response defined by (7), the maximum control force for unit-step command change (1 cm) can be found from Fig. 2, (12), and (7) to be

$$I_{q,\max} = \frac{M\mu_{dr}^2}{K_tK_x}. \quad (34)$$

This is the maximum value under the given mass and the defined tracking response. According to (34) and the pulsed current ratings of inverter and motor, the largest magnitude of step command can be determined. Exceeding this, the ramp command with suitable ramping rate should be adopted instead.

Comments and the Determination of w: Equation (32) and Fig. 5(b) indicate that the effects of parameter variations and force disturbance have been reduced by a factor of $(1-w(s))$. And the ideal control is obtained for $w(s) = w = 1$. However, some problems will occur for the larger value of w being chosen: i) the control current with larger value and changing rate will be resulted, this will let to the difficulty in achieving excellent current control performance experimentally; ii) the noise sensitivity of Δn shown in Fig. 2 in high-frequency range will become larger; and iii) the controlled system may become unstable for the existence of system nonlinearities, the most commonly encountered one is dead-time element, or called transport delay.

To consider the effect of system dead-time, let the plant model $G_p(s)$ in Fig. 2 be replaced by

$$G_p(s) = \frac{1}{Ms+D}e^{-\tau_d s} \approx \frac{1}{Ms+D}\frac{1-0.5\tau_d s}{1+0.5\tau_d s}. \quad (35)$$

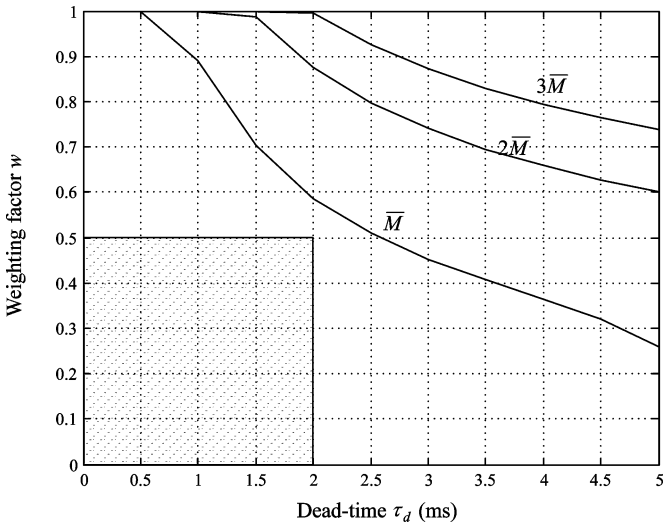

Fig. 6. Stability limits for w under various values of M and τ_d.

Through computer-aided analysis, the stability limits for various values of w, M and dead-time τ_d are plotted in Fig. 6. From the measured results shown in Fig. 4(a), one can be aware that the dead-time in this plant is about $\tau_d \approx 2.0$ ms. It follows that the weighting factor $w = 0.5$ is reasonably chosen for the mass varying range of $\overline{M} \le M \le 3\overline{M}$. Further analysis finds that the phase margin at the case of ($M = \overline{M}$, $\tau_d = 2$ ms and $w = 0.5$) is 48.7°.

B. Adapted Command Feedforward Control Scheme

It is obvious from the robust control presented above that the ideal command feedforward control can not be achieved for the chosen weighting function $w(s) = w/(1+\tau s)$, $0 \le w < 1$. To improve this, the parameters of the compensated motor drive are estimated and utilized to modify the inverse model parameters being set in the FFC.

From Fig. 5(b), one can find the equivalent plant model after adding the robust controller

$$G_p'(s) = \frac{1}{(\overline{M}s+\overline{D})+(1-w(s))(\Delta Ms+\Delta D)}. \quad (36)$$

For main dynamic frequency signals, $w(s) \approx w$ can be reasonably assumed. It follows that (36) can be approximated to be

$$G_p'(s) \approx \frac{1}{(\overline{M}+(1-w)\Delta M)s+(\overline{D}+(1-w)\Delta D)} \triangleq \frac{b'}{s+a'} \quad (37)$$

where $a' \triangleq D_{eq}/M_{eq}$ and $b' \triangleq 1/M_{eq}$ with $M_{eq} \triangleq \overline{M} + (1-w)\Delta M$ and $D_{eq} \triangleq \overline{D} + (1-w)\Delta D$ being the equivalent mass and damping ratio of the motor drive after applying robust control. Thus according to the inverse of $G_p'(s)$, the model parameters set in (11) of the FFC are updated real-time based on the identified values of ΔM and ΔD.

Parameter Identification From Estimated Disturbance Signal: Fig. 2 indicates that the estimated disturbance $\Delta\varepsilon_d$ contains the information of the parameter changes ΔM and

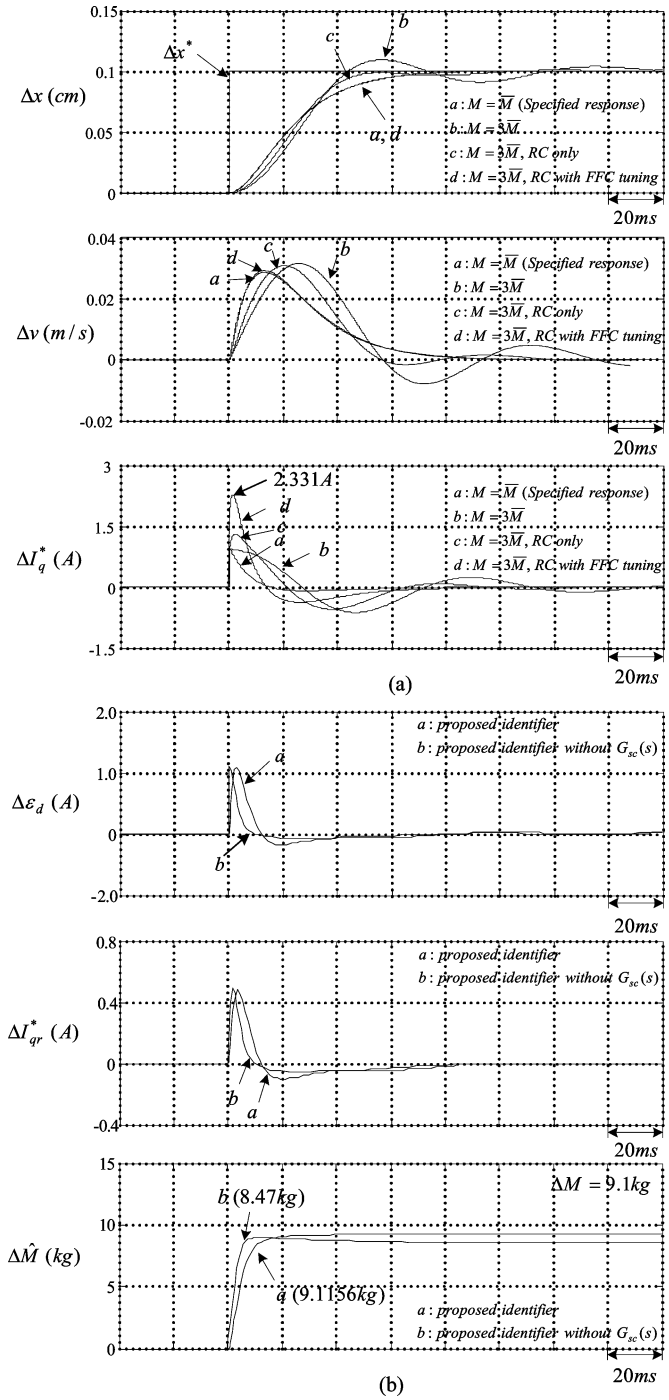

Fig. 7. Simulated results at $M = 3\overline{M}$ ($\overline{M} = 4.55$ kg): (a) responses due to a step position command change of 0.1 cm and (b) estimated disturbance $\Delta\varepsilon_d$, compensation control current ΔI^*_{qr} and identified mass $\Delta\hat{M}$ by the proposed method.

ΔD. During tracking control, $\Delta F_{Ld} = 0$, the governing equation of the proposed disturbance observer shown in Fig. 2 can be written as

$$K_t\Delta\varepsilon_d(t) + K_t\tau\frac{d\varepsilon_d(t)}{dt} = \Delta M\frac{d}{dt}\Delta v(t) + \Delta D\Delta v(t) + e(t) \tag{38}$$

where $e(t)$ denotes the model error. For avoiding the use of $dv(t)/dt$ and reducing the effect of system noise, the parameter identification can be made using the integration of $\Delta\varepsilon_d(t)$.

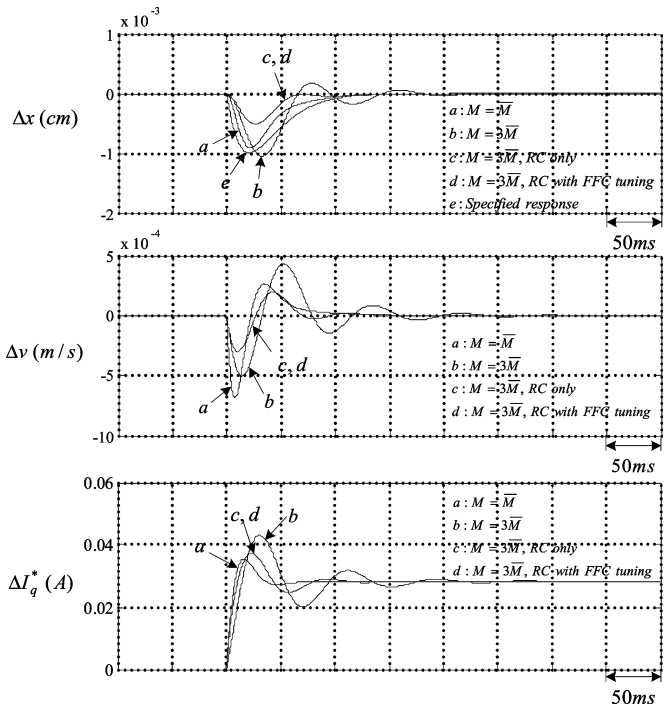

Fig. 8. Simulated position, velocity, and current responses of different control schemes at $M = 3\overline{M}$ ($\overline{M} = 4.55$ kg) due to a step load force change of 1 Nt.

Accordingly, define $\Delta\varepsilon_{dI}(t) \triangleq \int (K_t\Delta\varepsilon_d(t))dt$ and (38) is rewritten as

$$y(t) = \Theta(t)\Psi(t) + e(t) \tag{39}$$

where $y(t) \triangleq \Delta\varepsilon_{dI}(t) + K_t\tau\varepsilon_d(t)$, $\Theta(t) \triangleq [\Delta M, \Delta D]$ and $\Psi(t) \triangleq [\Delta v(t), \Delta x(t)]^T$. The recursive parameter estimates can be found as

$$\hat{\Theta}(t) = \hat{\Theta}(t-1) + K(t)(y(t) - \hat{y}(t)),\ \hat{y}(t) = \hat{\Theta}(t-1)\Psi(t). \tag{40}$$

The tuning gain $K(t)$ can be found applying various existing methods [24], such as Kalman filter approach, recursive least-squares approach, etc.

If only the mass change has occurred, the parameter identification process has degenerated to

$$\begin{aligned}\Delta\hat{M}(t) &= \Delta\hat{M}(t-1) + K(t)(y(t) - \hat{y}(t))\\ \hat{y}(t) &= \Delta\hat{M}(t-1)\Delta v(t).\end{aligned} \tag{41}$$

The excellent tracking control performance will be demonstrated by some simulation and experimental results presented as followed. The 2-norm of the position tracking error $\|\Delta\varepsilon_x(t)\|_2 \triangleq \left(\int_0^\infty |\varepsilon_x(t)|^2\,dt\right)^{1/2}$ is used as the control performance evaluation index.

C. Results

Fig. 7(a) shows the simulated position, velocity and current responses of different control schemes with $M = 3\overline{M}$ ($\overline{M} = 4.55$ kg) due to the step position command change (0.1 cm). For the convenience of comparison, the reference response trajectory ($M = \overline{M}$, curve a) is also plotted. The control schemes include: i) curve b: 2DOFC only; ii) curve c: 2DOFC

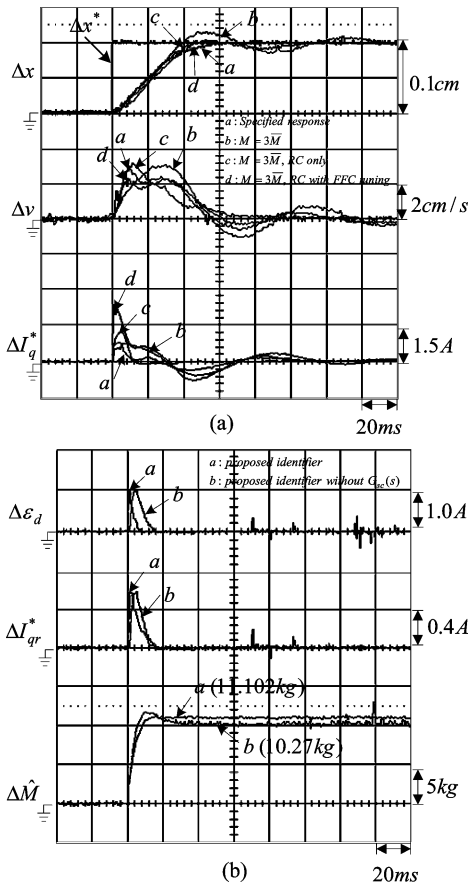

Fig. 9. (a) Measured Δx, Δv, and ΔI_q^* by different control schemes at $M = 3.435\overline{M}$ ($\overline{M} = 4.55$ kg) due to a step position command change of 0.1 cm and (b) measured key variables of the proposed identifier.

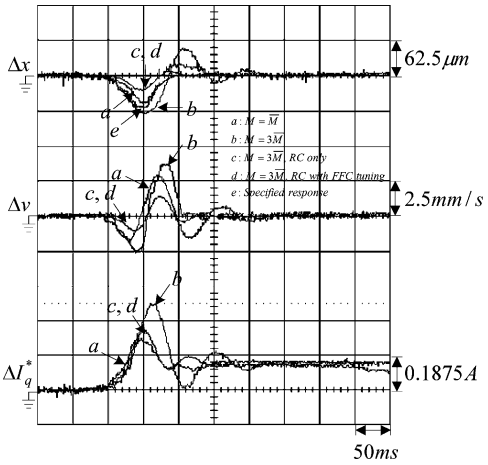

Fig. 10. Measured Δx, Δv and ΔI_q^* by different control schemes at $M = 3.435\overline{M}$ ($\overline{M} = 4.55$ kg) due to a step load force change of 5.316 Nt.

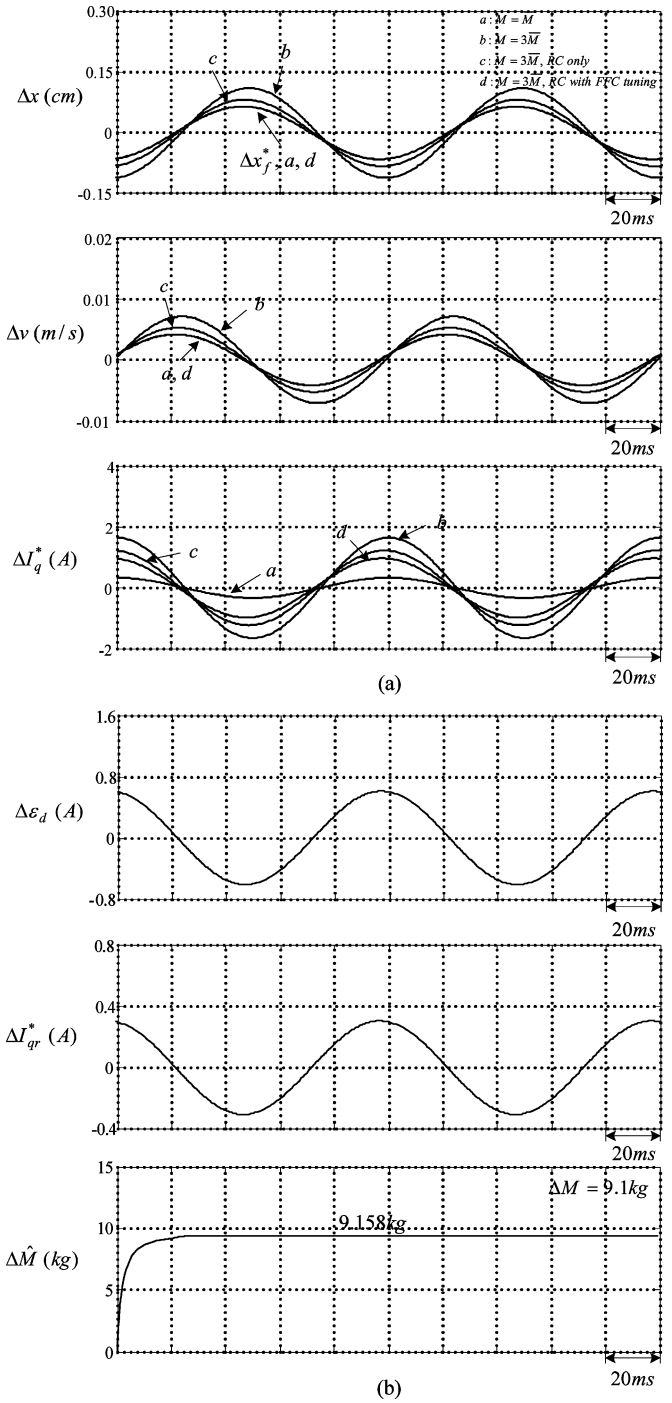

Fig. 11. Simulated results at $M = 3\overline{M}$ ($\overline{M} = 4.55$ kg): (a) responses corresponding to a sinusoidal position command with frequency = 10 Hz and amplitude = 0.1 cm and (b) estimated disturbance $\Delta\varepsilon_d$, compensation control current ΔI_{qr}^* and identified mass $\Delta\hat{M}$ by the proposed method.

and RC ($w(s) = 0.5/(1 + 0.001\text{s})$); and iii) curve d (the proposed scheme): 2DOFC with adapted FFC tuning and RC ($w(s) = 0.5/(1 + 0.001\text{s})$). Further computation indicates that the $\|\Delta\varepsilon_x(t)\|_2$ corresponding to these three curves respectively are 0.0314, 0.0141, and 0.0016. The 2-norm of the position tracking error is significantly reduced by the proposed control approach. From Fig. 7(a), the maximum value of current command is $\Delta I_{q\max}^* = 2.331$ A, which is close to the estimated one listed in (34). Fig. 7(b) further shows the estimated disturbance $\Delta\varepsilon_d$, the compensation control current ΔI_{qr}^* and the estimated mass $\Delta\hat{M}$ by the proposed method (the curves labeled by "a"). One can observe that quick and accurate estimation of $\Delta\hat{M}$ is obtained. Now let $G_{sc}(s) = 1$ is set, the estimated result of $\Delta\hat{M}$ (the curves labeled by "b") indicates that there exists a slight estimation error, which is mainly due to the nonideal differentiator ($s \to s/(1 + \tau s)$) being adopted. The position tracking response (not shown here) indicates that $\|\Delta\varepsilon_x(t)\|_2 =$

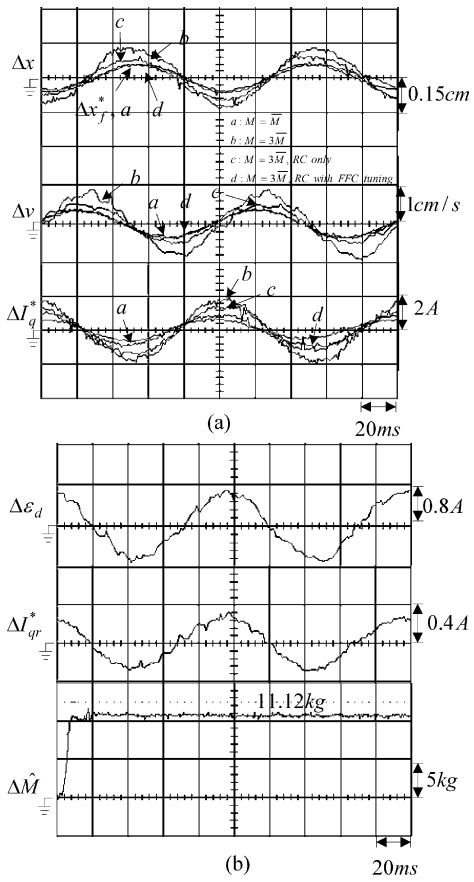

Fig. 12. (a) Measured Δx, Δv and ΔI_q^* by different control schemes at $M = 3.435\overline{M}$ ($\overline{M} = 4.55$ kg) corresponding to a sinusoidal position command with frequency = 10 Hz and amplitude = 0.1 cm and (b) measured key variables of the proposed identifier.

0.0028 in this case. The estimated error can be eliminated by adding the proposed signal conditioning compensator $G_{sc}(s)$.

Fig. 8 shows the simulated responses with $M = 3\overline{M}$ by various control schemes due to a step load force change of 1 Nt. Good position regulation control performance in smaller dip and faster restoration by the proposed control scheme can be observed from the results.

Let $\Delta M = 11.08$ kg ($\approx 2.435\overline{M}$) be added to the positioning stage, the measured responses due to step position command change (0.1 cm) by the 2DOFC only are shown in Fig. 9(a) (curves b). Bad tracking control characteristic is observed. Now let the robust control with $w(s) = 0.5/(1 + 0.001\text{s})$ be applied, the measured results are plotted in Fig. 9(a) (curves c). Although some extent of improvement in dynamic responses has been seen, it is still far from ideal. To improve this, let the FFC be tuned online via the proposed self-tuning adaptive control approach, the measured results shown in Fig. 9(a) (curves d) clearly indicate that excellent position model following response has been achieved. The measured key variables of the proposed identifier are plotted in Fig. 9(b), the accurate estimated $\Delta\hat{M}$(= 11.102 kg) obtained by adding $G_{sc}(s)$ is observed.

The measured responses due to a step load force change (0 Nt to 5.316 Nt) by the 2DOFC without and with robust control ($w(s) = 0.5/(1 + 0.001\text{s})$) are compared in Fig. 10. By normalizing the measured results by a factor of 5.316 and comparing with the simulated results shown in Fig. 8, the similar comments to those being made previously for Figs. 3(b) and 4(b) can also be given. The results in Fig. 10 also indicate that the position regulation control responses are much improved by applying the proposed robust control.

For further confirming the effectiveness and performance of the proposed control approach, Figs. 11(a) and (b) and 12(a) and (b), respectively, show the simulated and measured tracking responses corresponding to a sinusoidal position command with frequency = 10 Hz and amplitude = 0.1 cm at the same conditions of those in Figs. 7 and 9. The results can also confirm the effectiveness of the proposed control scheme in control performance improvement and accurate parameter identification.

V. Conclusion

The adaptive positioning control for an LPMSM drive based on an adapted inverse model and a robust disturbance observer has been presented in this paper. At nominal case, the 2DOFC is first designed to meet the given tracking and regulation control specifications. The major features of the proposed 2DOFC lie in: i) avoiding the use of pure differentiation in the FFC (this is a common problem possessed by the traditional control scheme) and ii) in the design of a FBC to handle the quantitative regulation control as the model reduction concept is employed to treat a high-order dynamic process. In handling the robust and quantitative control under varied cases, the key methodologies proposed in this paper are: i) the effects of system parameter changes and disturbances are first reduced as far as possible using a disturbance observer based robust cancellation control scheme whose weighting function is properly determined considering the effect of system dead-time and ii) the nonideal robust control in tracking performance (this is common for the existing scheme) is then improved via the proposed self-tuning adapted FFC. The parameters set in the FFC are updated in real-time by the developed identifier, which performs the parameter identification using the observed system disturbance from the proposed robust controller. Effectiveness of the proposed control scheme has been demonstrated by simulated and experimental results.

Appendix
Motor Drive System Parameters

- LPMSM: rated continuous force = 80 lbs, peak force = 240 lbs.
- Inverter: i) constructed using insulated gate bipolar transistor (IGBT), ii) input source: ac 3ϕ 50/60 Hz (220 V$\sim$ 230 V) $\pm$ 10%), and iii) output power = 1 kW and output continuous current is 5 A_{RMS}, output peak current = 7.5 A/1 min.
- CCPWM scheme: PI controller with $G_{ci}(s) = 10 + 21\,276.6/\text{s}$.

References

[1] J. F. Gieras and Z. J. Piech, *Linear Synchronous Motors: Transportation and Automation Systems*. Boca Raton, FL: CRC Press, 2000.

[2] G. Brandenburg, S. Brűckl, J. Dormann, J. Heinzl, and C. Schmidt, "Comparative investigation of rotary and linear motor feed drive systems for high precision machine tools," in *Proc. IEEE 6th Int. Workshop Advanced Motion Control*, Mar.–Apr. 30–1, 2000, pp. 384–389.
[3] A. De Carli and R. Caccia, "A comparison of some control strategies for motion control," *Pergamon Mechatron.*, vol. 5, no. 1, pp. 61–71, 1995.
[4] K. Ohnishi, M. Shibata, and T. Murakami, "Motion control for advanced mechatronics," *IEEE/ASME Trans. Mechatron.*, vol. 1, no. 1, pp. 56–67, Mar. 1996.
[5] G. Ellis and R. D. Lorenz, "Comparison of motion control loops for industrial applications," in *Proc. IEEE 34th IAS Annu. Meeting*, Oct. 3–7, 1999, pp. 2599–2605.
[6] S. Komada, M. Ishida, K. Ohnishi, and T. Hori, "Motion control of linear synchronous motors based on disturbance observer," in *Proc. IEEE 16th Annu. Conf. Ind. Electron. Soc.*, vol. 1, Nov. 27–30, 1990, pp. 154–159.
[7] H. S. Lee and M. Tomizuka, "Robust motion controller design for high-accuracy positioning systems," *IEEE Trans. Ind. Electron.*, vol. 43, no. 1, pp. 48–55, Feb. 1996.
[8] C. H. Chen and H. Van Brussel, "Servo control of flexible beam with inverse-dynamics feedforward and disturbance observer," in *Proc. IEEE Int. Symp. Ind. Electron.*, Jun. 1–3, 1993, pp. 702–707.
[9] L. Guo and M. Tomizuka, "High-speed and high-precision motion control with an optimal hybrid feedforward controller," *IEEE/ASME Trans. Mechatron.*, vol. 2, no. 2, pp. 110–122, Jun. 1997.
[10] G. Otten, T. J. A. de Vries, J. van Amerongen, A. M. Rankers, and E. W. Gaal, "Linear motor motion control using a learning feedforward controller," *IEEE/ASME Trans. Mechatron.*, vol. 2, no. 3, pp. 179–187, Sep. 1997.
[11] F. Fujimoto, Y. Hori, T. Yamaguchi, and S. Nakagawa, "Proposal of perfect tracking and perfect disturbance rejection control by multirate sampling and applications to hard disk drive control," in *Proc. IEEE 38th Conf. Decision Control*, vol. 5, Dec. 7–10, 1999, pp. 5277–5282.
[12] K. K. Tan, S. Y. Lim, and S. N. Huang, "Two-degree-of-freedom controller incorporating RBF adaptation for precision motion control applications," in *Proc. IEEE/ASME Int. Conf. Advanced Intelligent Mechatron.*, Sep. 19–23, 1999, pp. 848–853.
[13] C. M. Liaw, R. Y. Shue, H. C. Chen, and S. C. Chen, "Development of a linear brushless dc motor drive with robust position control," *Proc. Inst. Elect. Eng.*, vol. 148, no. 2, pp. 111–118, Mar. 2001.
[14] K. K. Tan, T. H. Lee, H. F. Dou, S. J. Chin, and S. Zhao, "Precision motion control with disturbance observer for pulsewidth-modulated-driven permanent-magnet linear motors," *IEEE Trans. Magn.*, vol. 39, no. 3, pp. 1813–1818, May 2003.
[15] S. Komada, T. Kimura, M. Ishida, and T. Hori, "Robust position control of manipulators based on disturbance observer and inertia identifier in task space," in *Proc. 4th Int. Workshop Advanced Motion Control*, vol. 1, Mar. 18–21, 1996, pp. 225–230.
[16] S. Komada, K. Nomura, M. Ishida, K. Ohnishi, and T. Hori, "Adaptive robust force control by disturbance observer," in *Proc. Int. Conf. Ind. Electron., Control, Instrum. Automat.*, vol. 3, Nov. 9–13, 1992, pp. 1494–1499.
[17] Y. Bin, M. Al-Majed, and M. Tomizuka, "High-performance robust motion control of machine tools: An adaptive robust control approach and comparative experiments," *IEEE/ASME Trans. Mechatron.*, vol. 2, no. 2, pp. 63–76, Jun. 1997.
[18] K. H. Kim and M. J. Youn, "A nonlinear speed control for a PM synchronous motor using a simple disturbance estimation technique," *IEEE Trans. Ind. Electron.*, vol. 49, no. 3, pp. 524–535, Jun. 2002.
[19] A. Rojko and K. Jezernik, "Sliding-mode motion controller with adaptive fuzzy disturbance estimation," *IEEE Trans. Ind. Electron.*, vol. 51, no. 5, pp. 963–971, Oct. 2004.
[20] T. Miyazaki, K. Ohishi, K. Inomata, K. Kuramochi, D. Koide, and D. Tokumaru, "Robust feedforward tracking control based on sudden disturbance observer and ZPET control for optical disk recording system," in *Proc. 8th IEEE Int. Workshop Advanced Motion Control*, Mar. 25–28, 2004, pp. 353–358.
[21] K. K. Tan, S. Zhao, and S. Huang, "Iterative reference adjustment for high-precision and repetitive motion control applications," *IEEE Trans. Contr. Syst. Technol.*, vol. 13, no. 1, pp. 85–97, Jan. 2005.
[22] F. Moynihan, "Fundamentals of DSP-based control for ac machines," *Analog Dialogue*, vol. 34, no. 6, pp. 1–7, Oct. 2000.
[23] C. M. Liaw, "System parameter estimation from sampled data," in *Control and Dynamic Systems*. New York: Academic, 1994, vol. 63, pp. 161–195.
[24] R. Johansson, *System Modeling and Identification*. Englewood Cliffs, NJ: Prentice-Hall, 1993.

Wei-Te Su was born in Taiwan, R.O.C., on September 18, 1977. He received the B.S. and the M.S. degrees in electrical engineering from National Tsing Hua University, Hsinchu, Taiwan, in 1999 and 2001, respectively, where he is currently pursuing the Ph.D. degree in the Department of Electrical Engineering.

His areas of research are power electronics, servo control, and motor drives.

Chang-Ming Liaw (S'88–M'89) was born in Taichung, Taiwan, R.O.C., on June 19, 1951. He received the B.S. degree in electronic engineering from Tamkang College of Arts and Sciences, Taipei, Taiwan, in 1979 and the M.S. and Ph.D. degrees in electrical engineering from National Tsing Hua University, Hsinchu, Taiwan, in 1981 and 1988, respectively.

In 1988, he joined the faculty of National Tsing Hua University as an Associate Professor in electrical engineering. Since 1993, he has been a Professor in the Department of Electrical Engineering. His areas of research interest are power electronics, motor drives, and electric machine control.

Dr. Liaw is a life member of the CIEE.